Electronic Supplementary Information

For

Aluminum Complexes of Phenoxy-Azo Ligands in Catalysis of *rac*-Lactide Polymerisation

Pattarawut Sumrit,[a,b] *Sirawan Kamavichanurat,*[a,b] *Wasan Joopor,*[a,b] *Worawat Wattanathana,*[c] *Chutikan Nakornkhet,*[a,b] *and Pimpa Hormnirun*[*,a,b]

[a]Laboratory of Catalysts and Advanced Polymer Materials, Department of Chemistry and Cente of Excellence for Innovation in Chemistry, Faculty of Science, Kasetsart University, Bangkok 10900, Thailand

[b]Centre for Advanced Studies in Nanotechnology for Chemical, Food and Agricultural Industries, Kasetsart University, Bangkok 10900, Thailand

[c]Department of Materials Engineering, Faculty of Engineering, Kasetsart University, Bangkok 10900, Thailand

*E-mail: fscipph@ku.ac.th

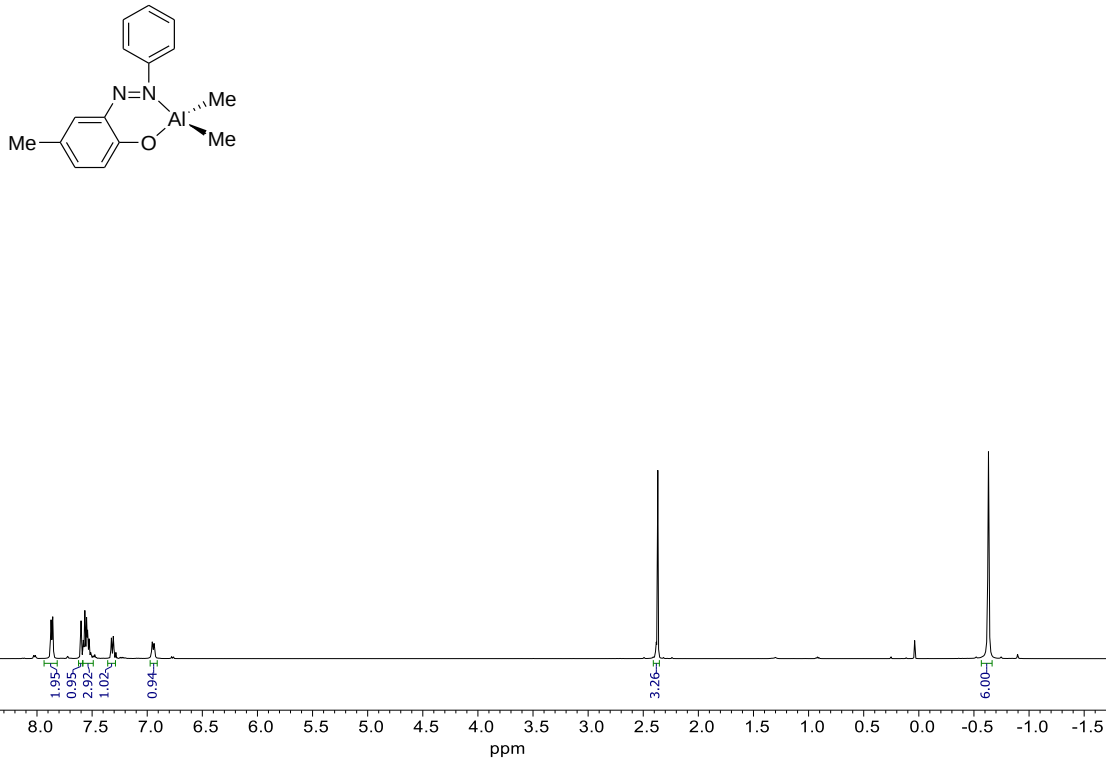

Fig. S1 ^{1}H NMR spectrum of **1a** in $CDCl_3$ at 298 K.

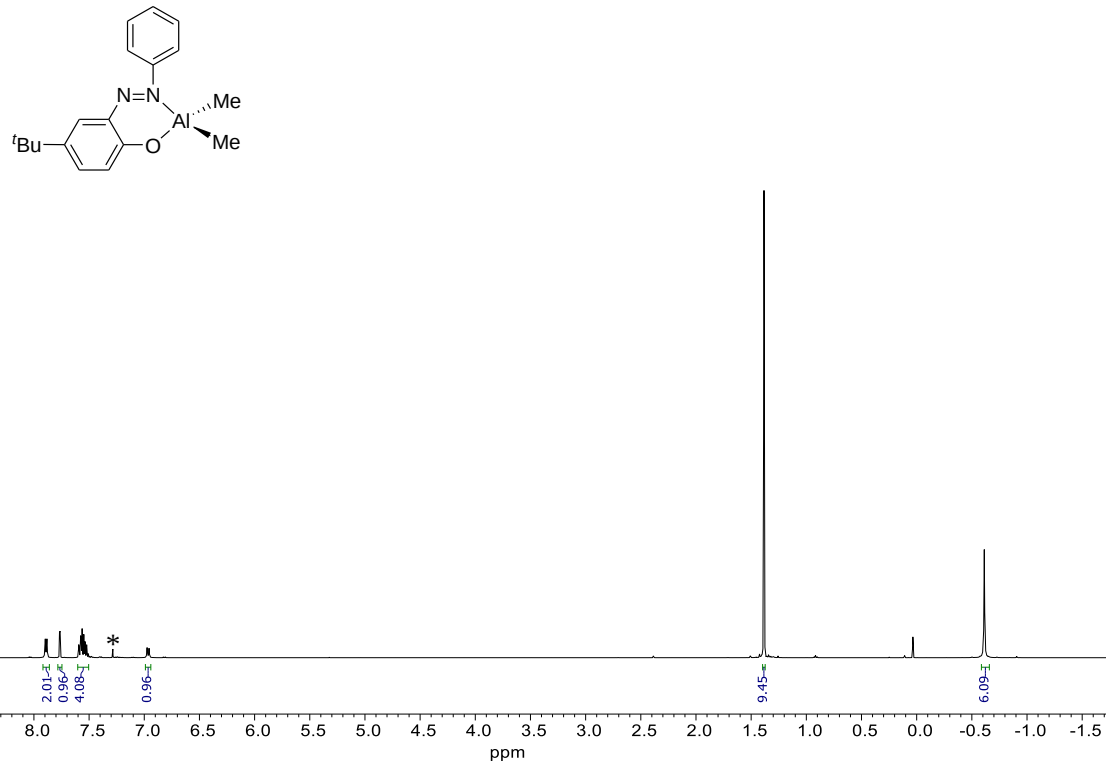

Fig. S2 ^{1}H NMR spectrum of **2a** in $CDCl_3$ at 298 K (* = solvent residue signal).

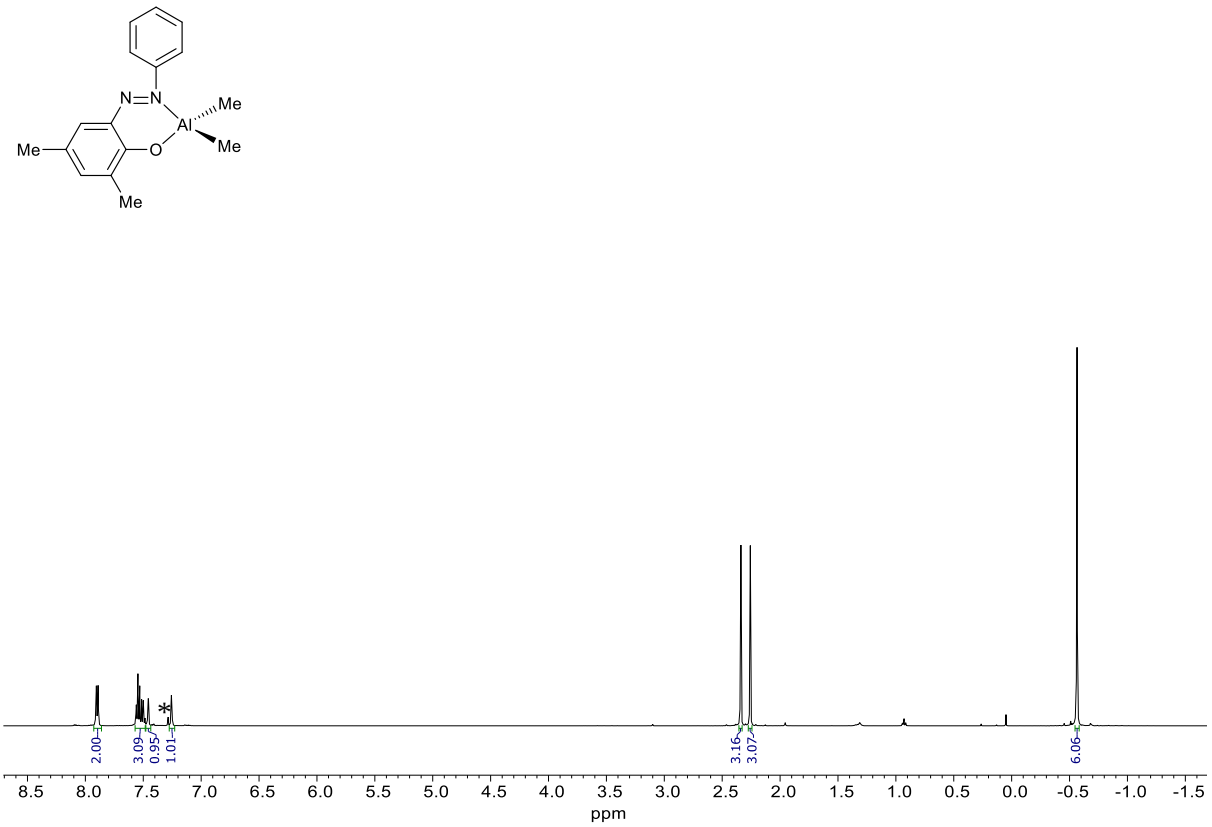

Fig. S3 ^{1}H NMR spectrum of **3a** in $CDCl_3$ at 298 K (* = solvent residue signal).

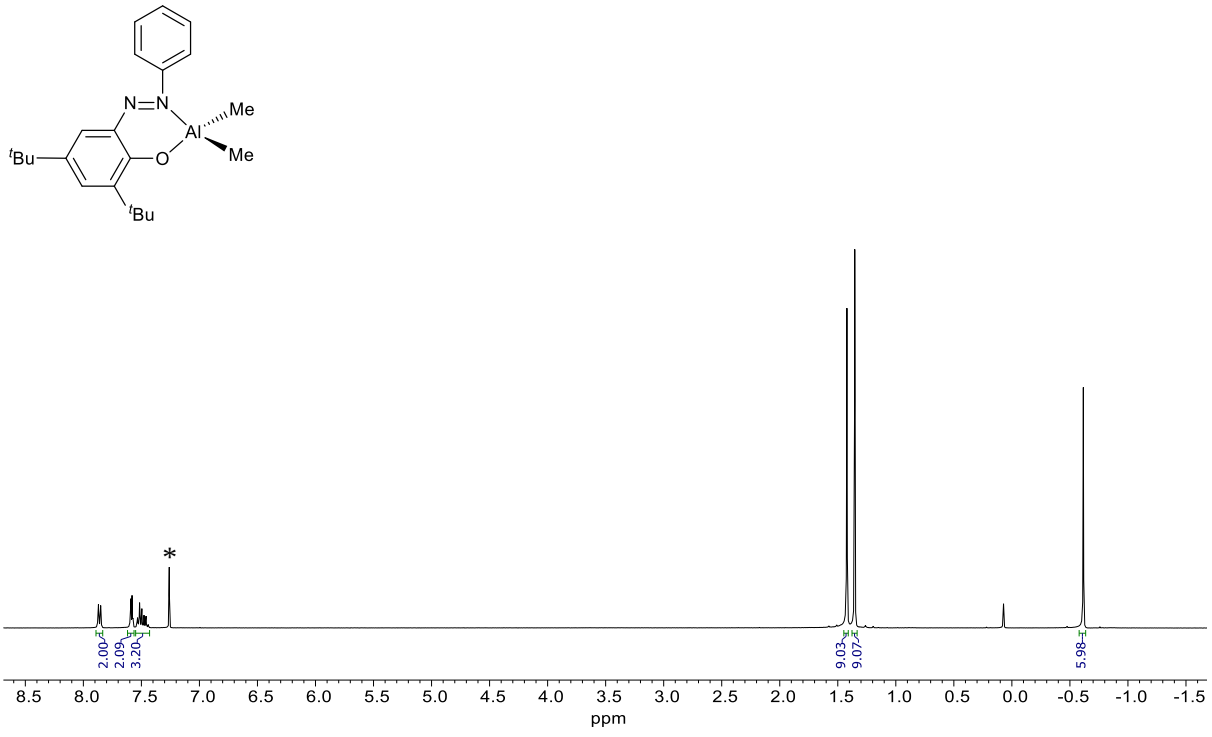

Fig. S4 ^{1}H NMR spectrum of **4a** in $CDCl_3$ at 298 K (* = solvent residue signal).

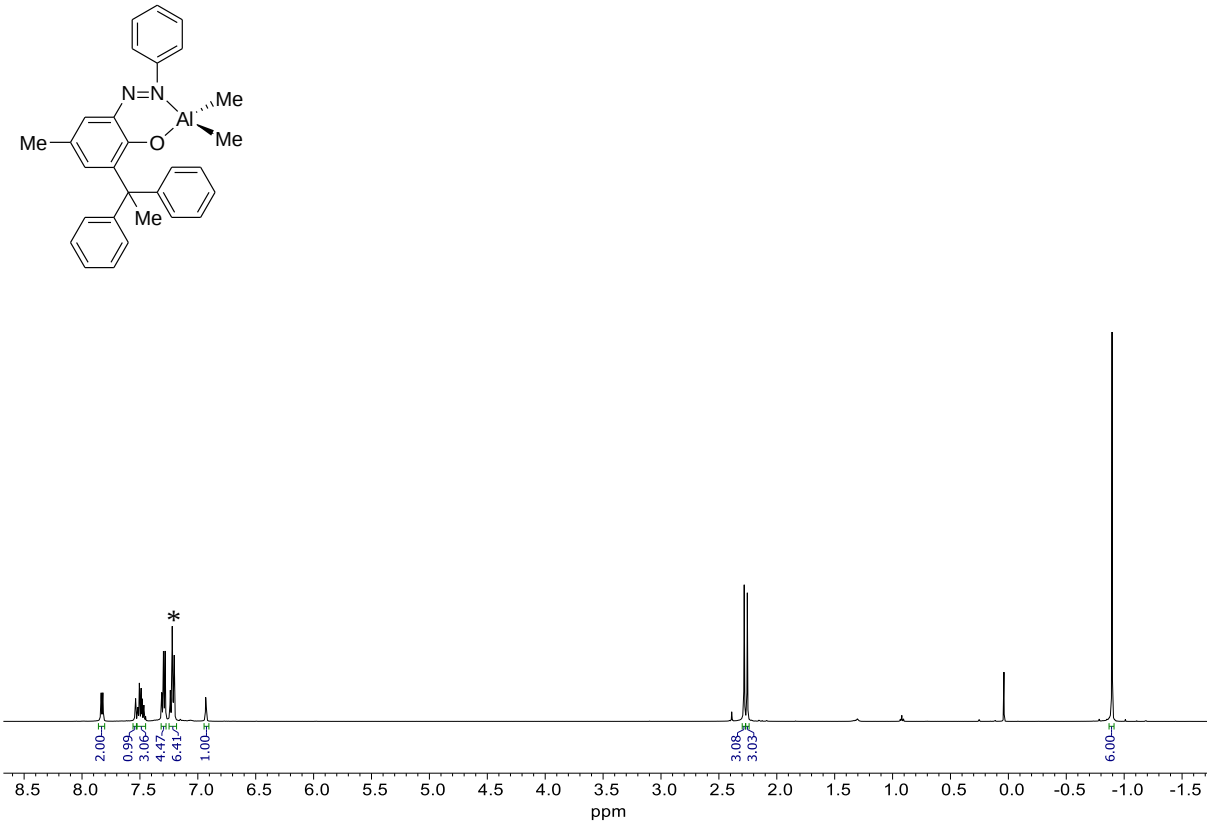

Fig. S5 ^{1}H NMR spectrum of **5a** in $CDCl_3$ at 298 K (* = solvent residue signal).

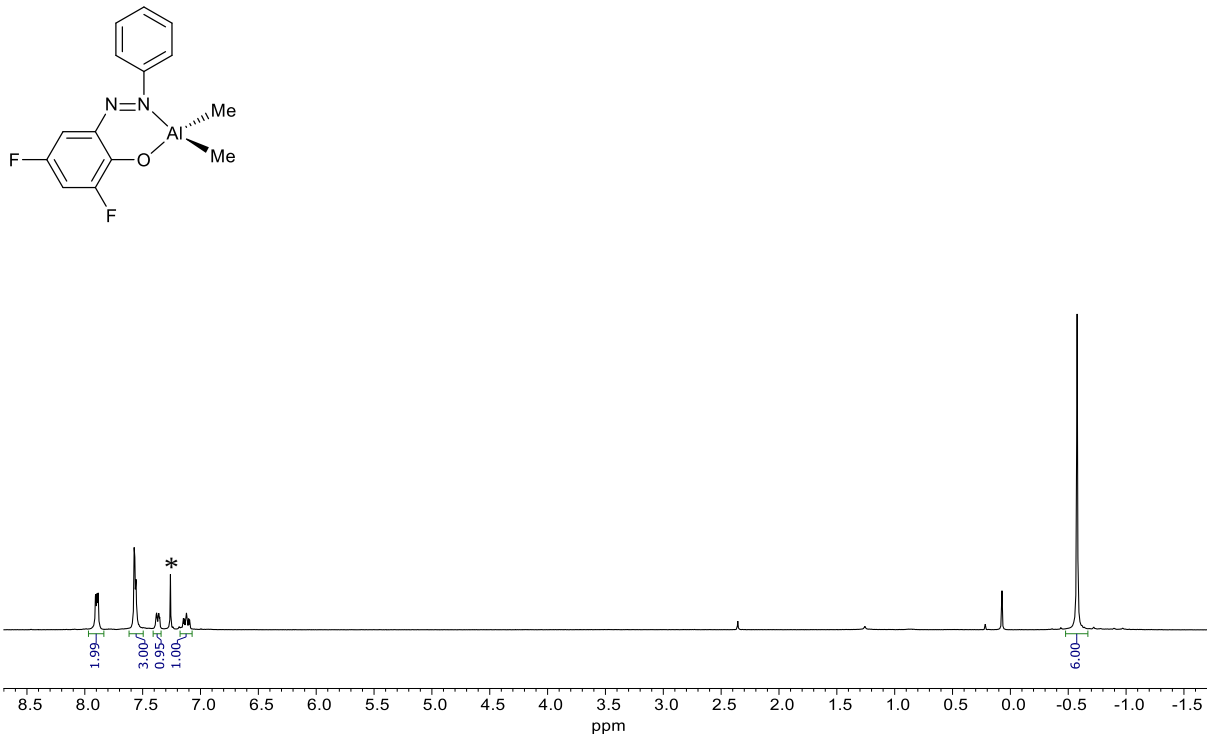

Fig. S6 ^{1}H NMR spectrum of **6a** in $CDCl_3$ at 298 K (* = solvent residue signal).

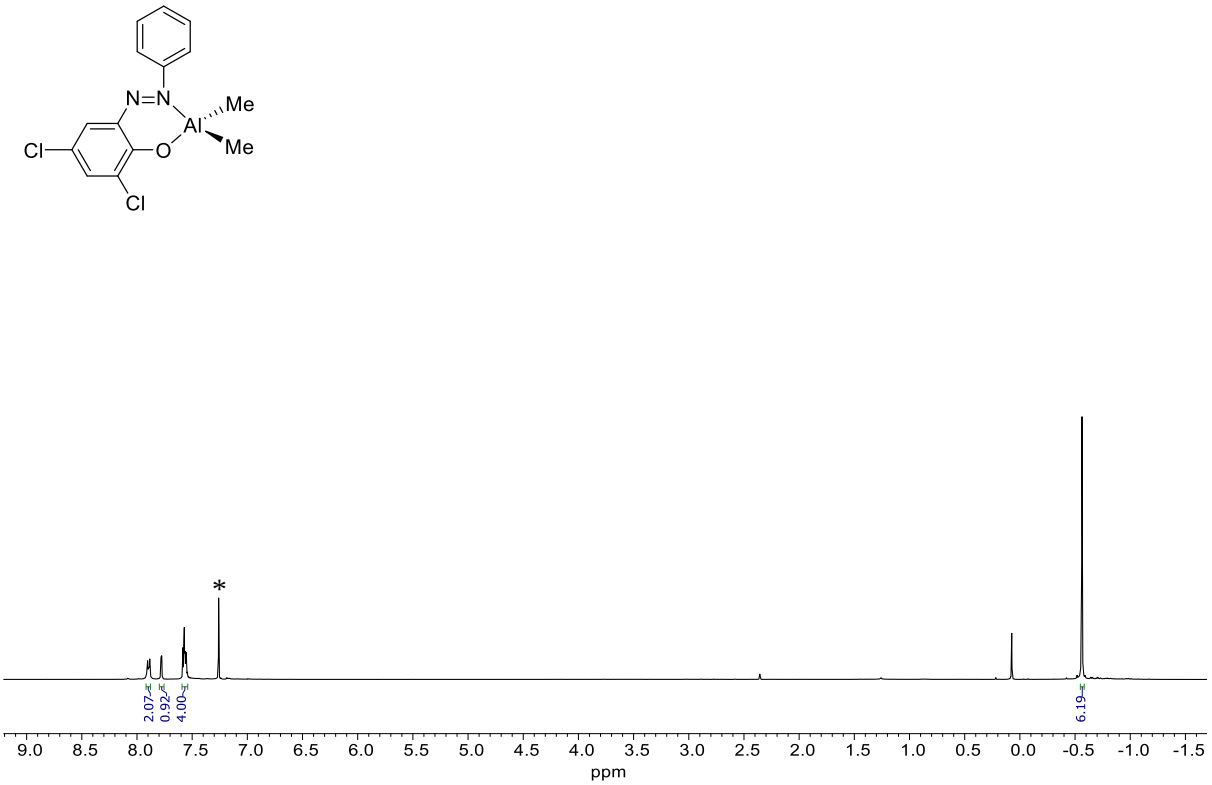

Fig. S7 ^{1}H NMR spectrum of **7a** in $CDCl_3$ at 298 K (* = solvent residue signal).

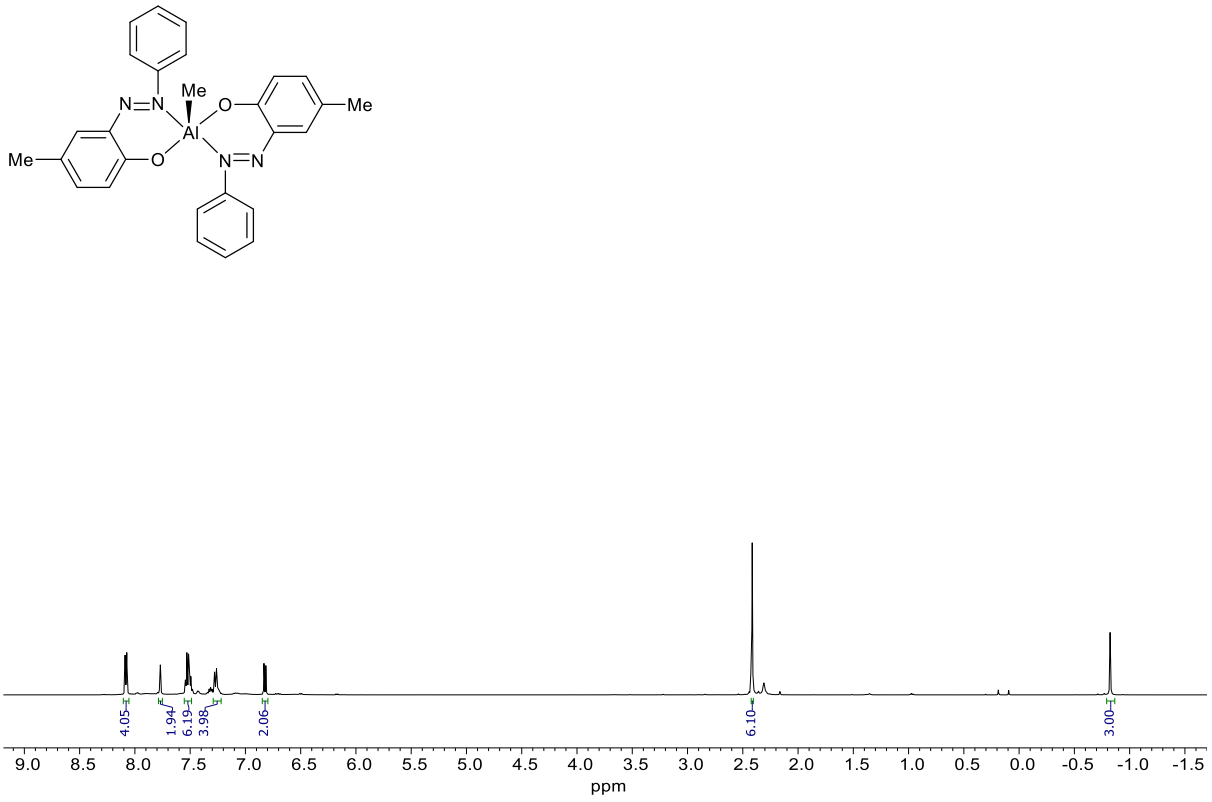

Fig. S8 ^{1}H NMR spectrum of **1b** in $CDCl_3$ at 298 K.

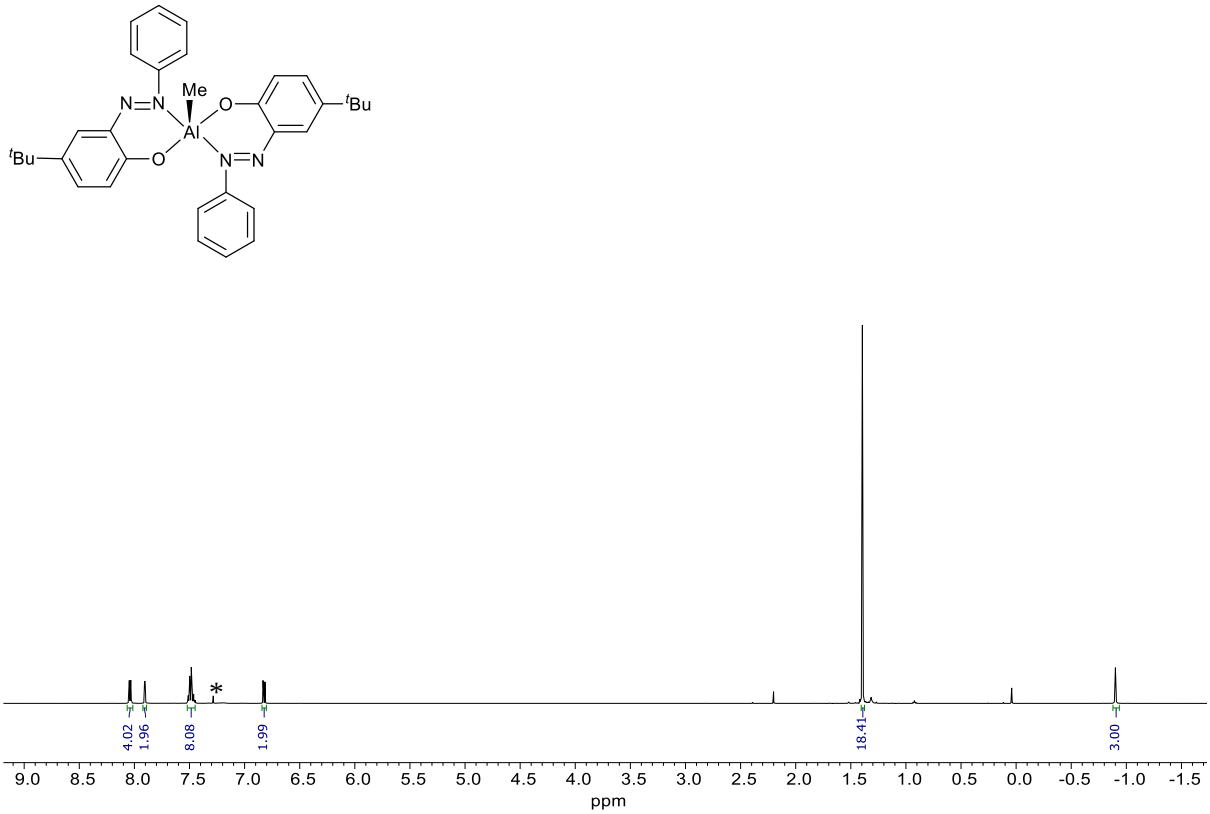

Fig. S9 ^{1}H NMR spectrum of **2b** in $CDCl_3$ at 298 K (* = solvent residue signal).

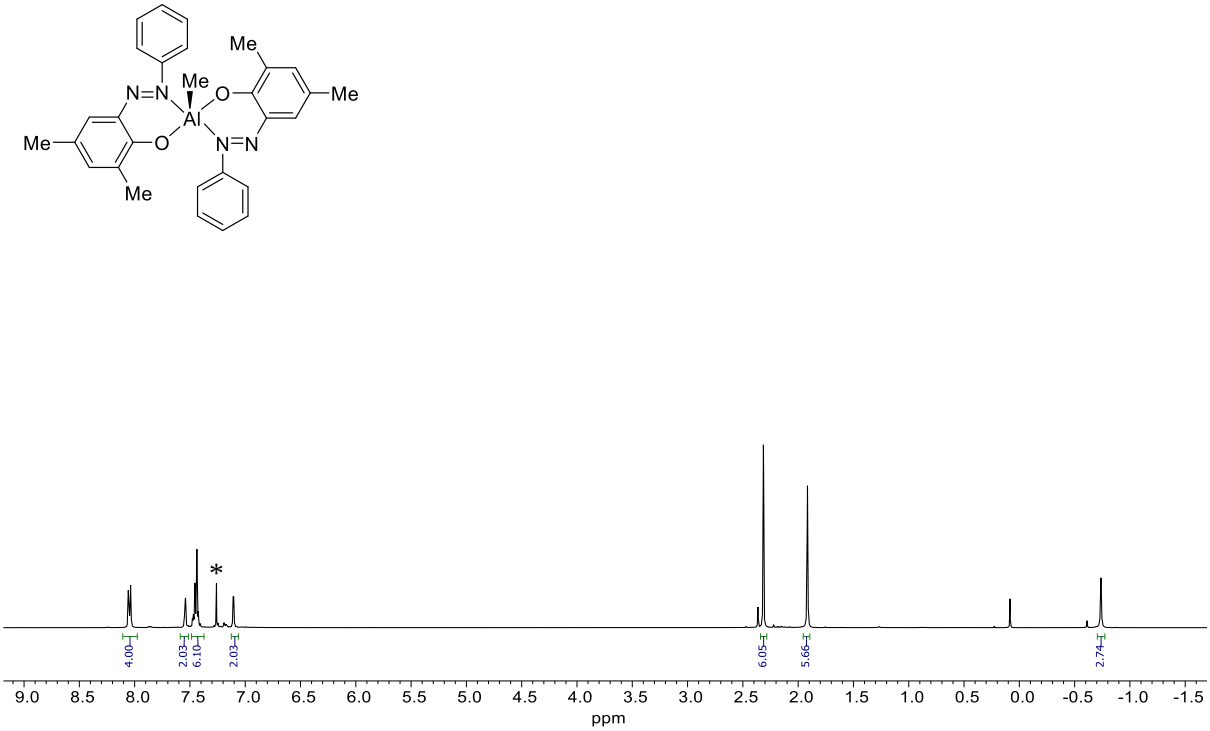

Fig. S10 ^{1}H NMR spectrum of **3b** in $CDCl_3$ at 298 K (* = solvent residue signal).

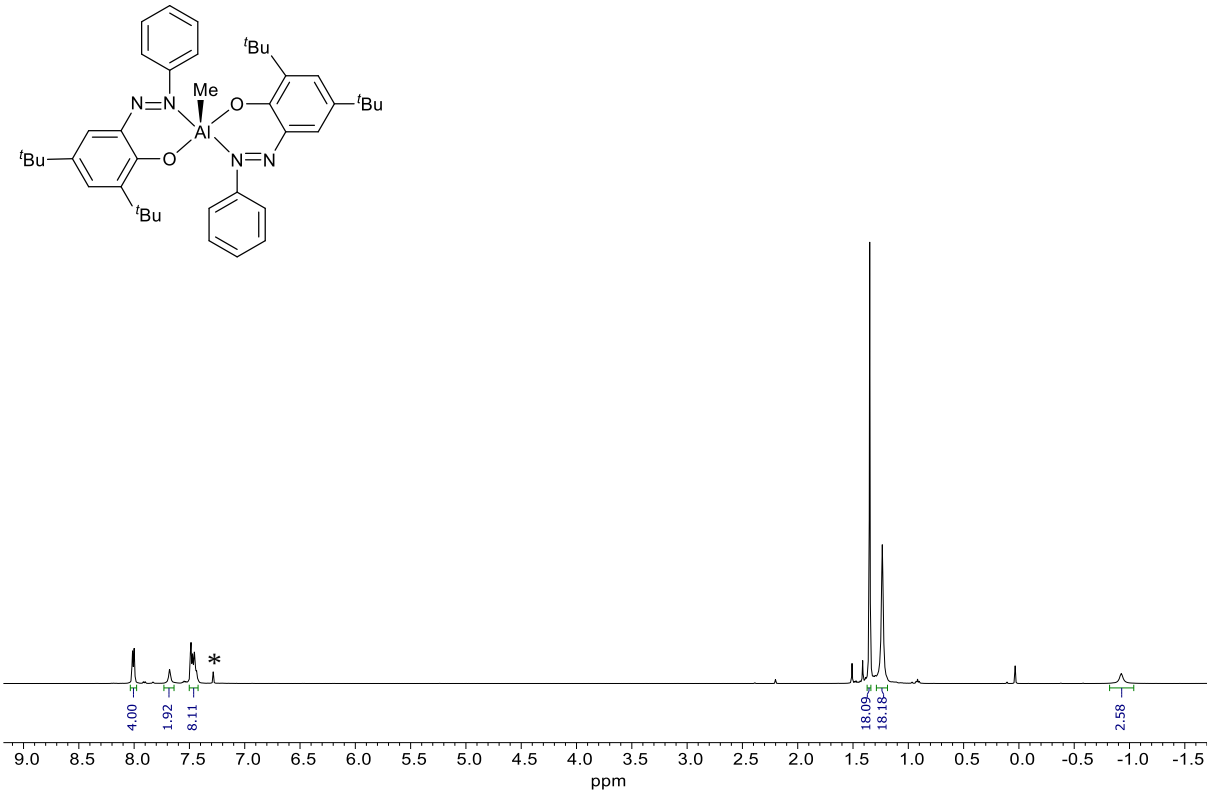

Fig. S11 ^{1}H NMR spectrum of **4b** in $CDCl_3$ at 298 K (* = solvent residue signal).

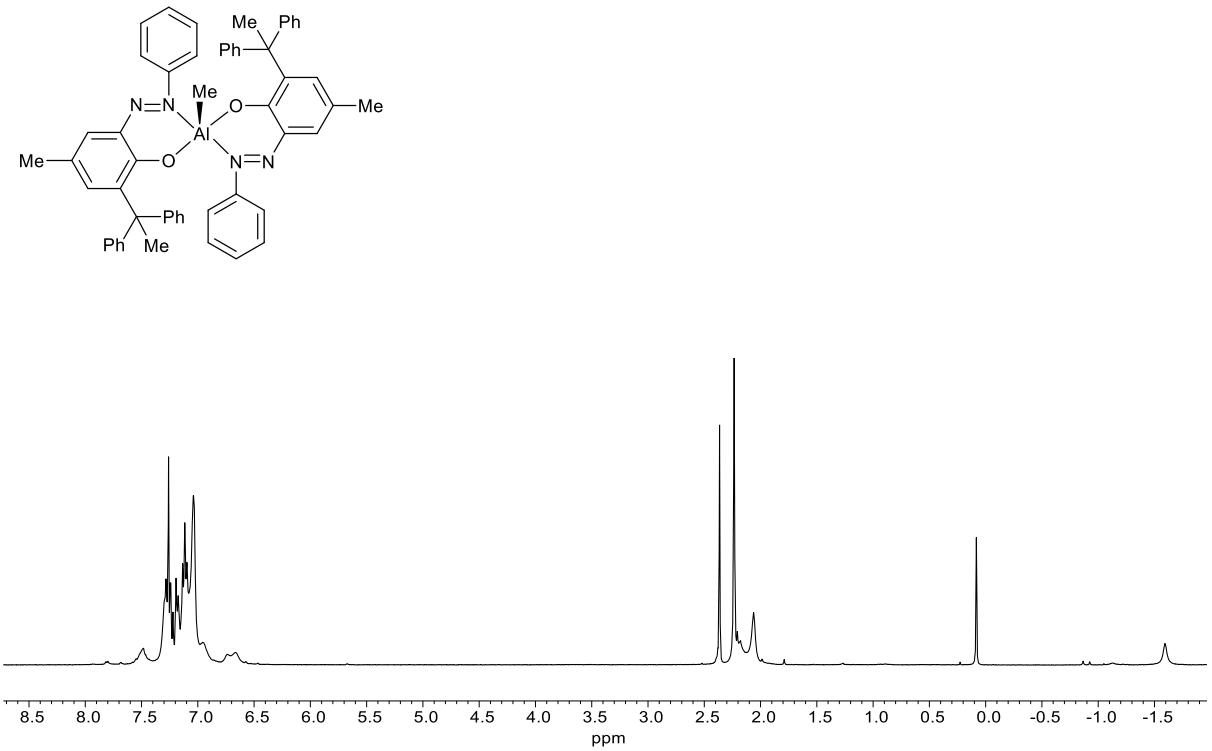

Fig. S12 ^{1}H NMR spectrum of **5b** in $CDCl_3$ at 298 K.

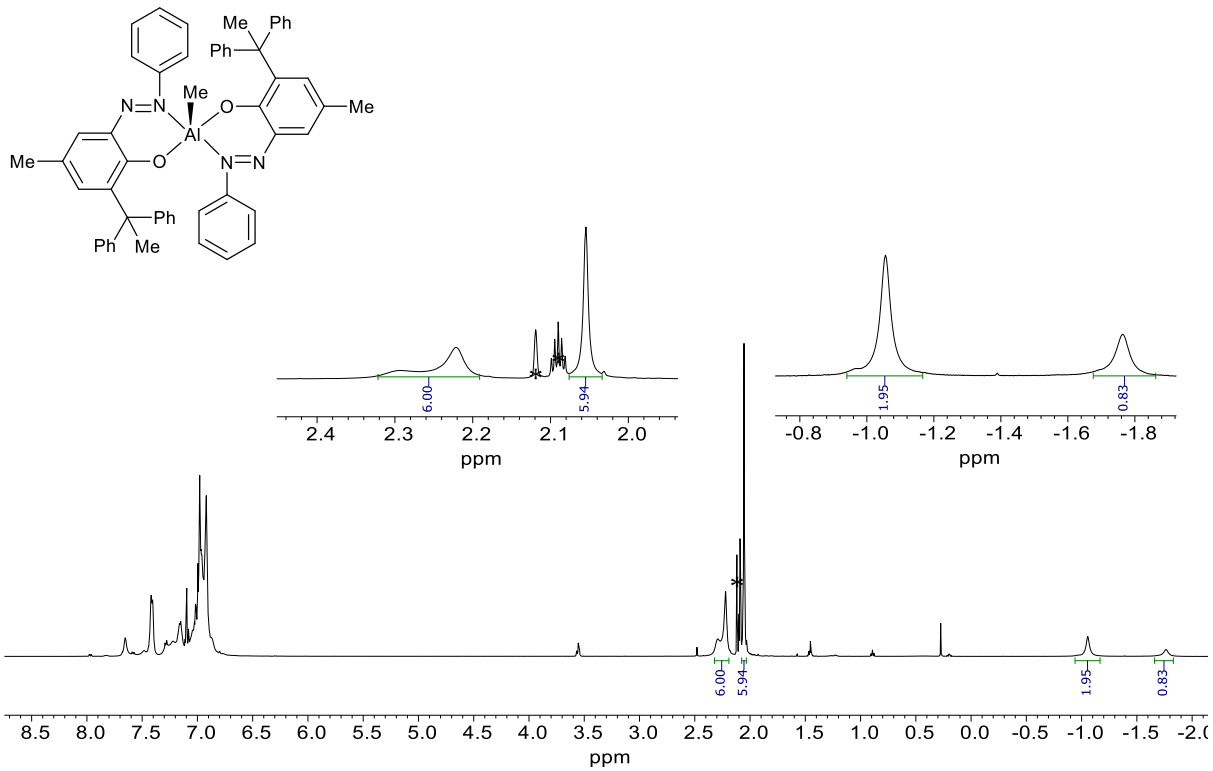

Fig. S13 ^{1}H NMR spectrum of **5b** in toluene-d_8 at 298 K (* = solvent residue signal).

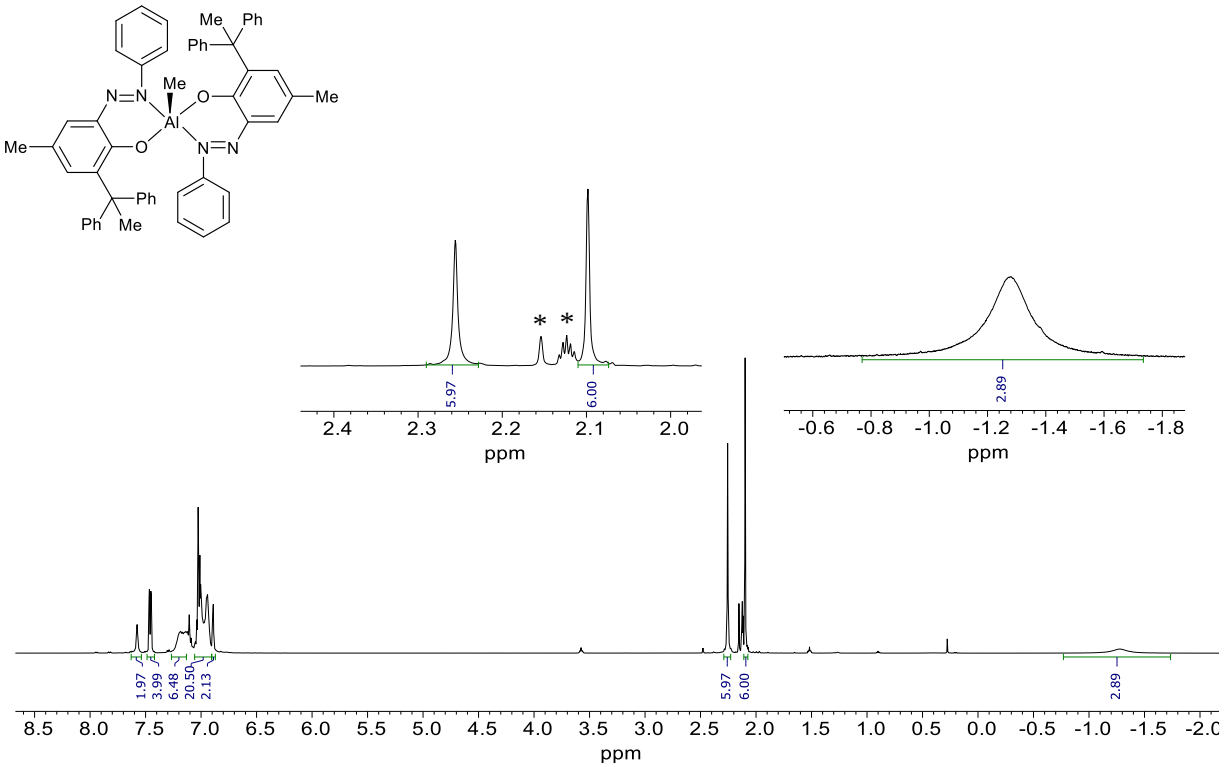

Fig. S14 ^{1}H NMR spectrum of **5b** in toluene-d_8 at 343 K (* = solvent residue signal).

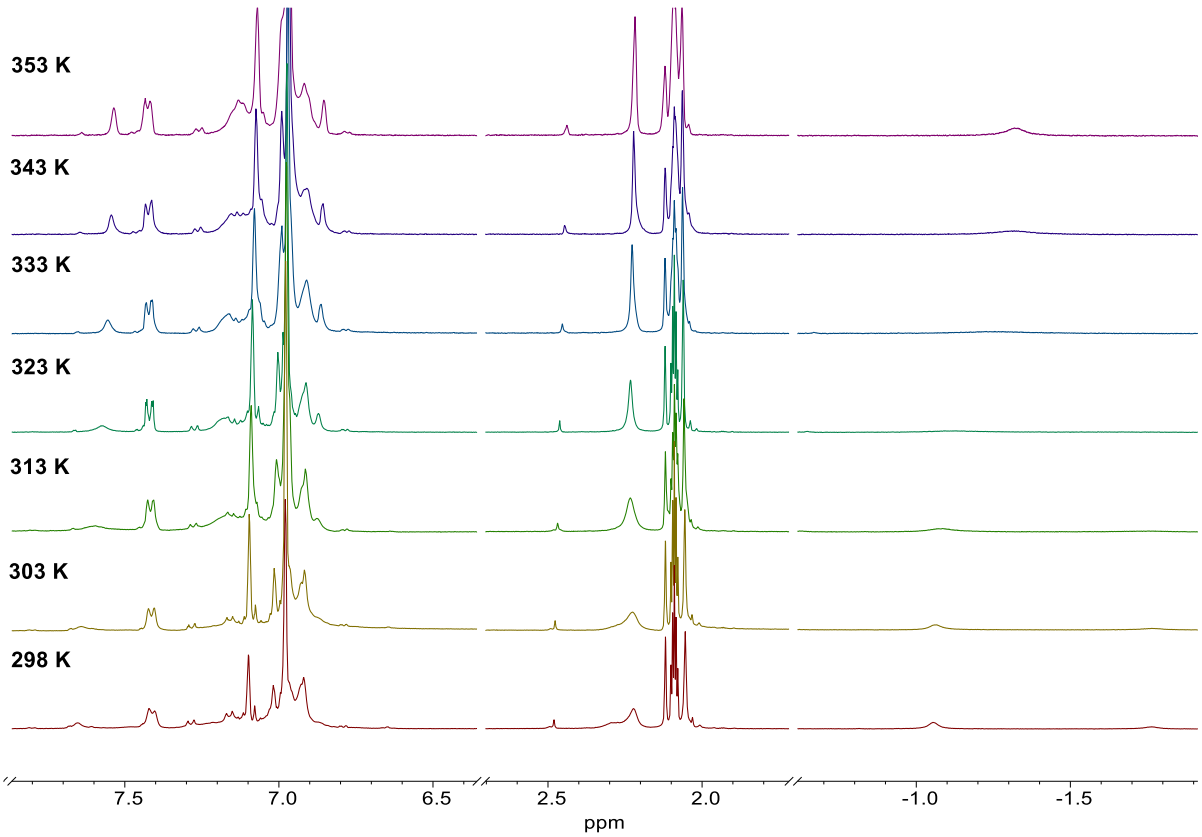

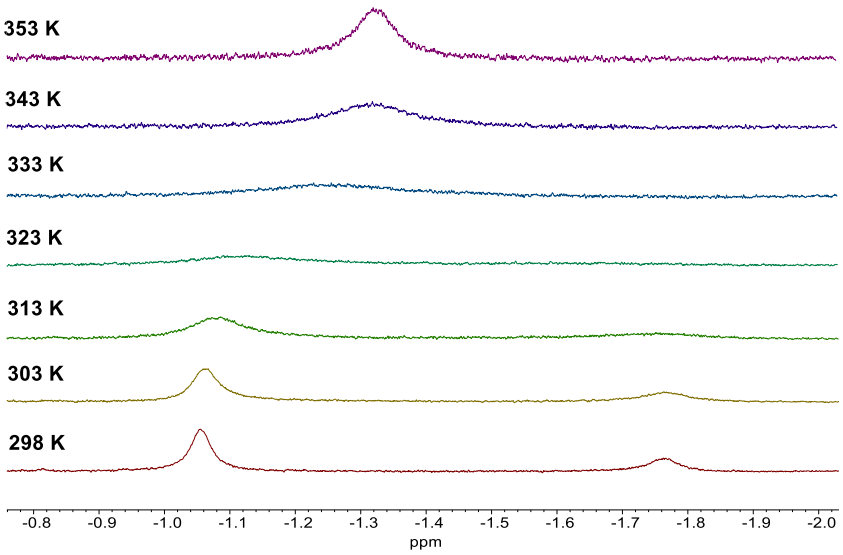

Fig. S15 VT ^{1}H NMR spectra of **5b** in toluene-d_8.

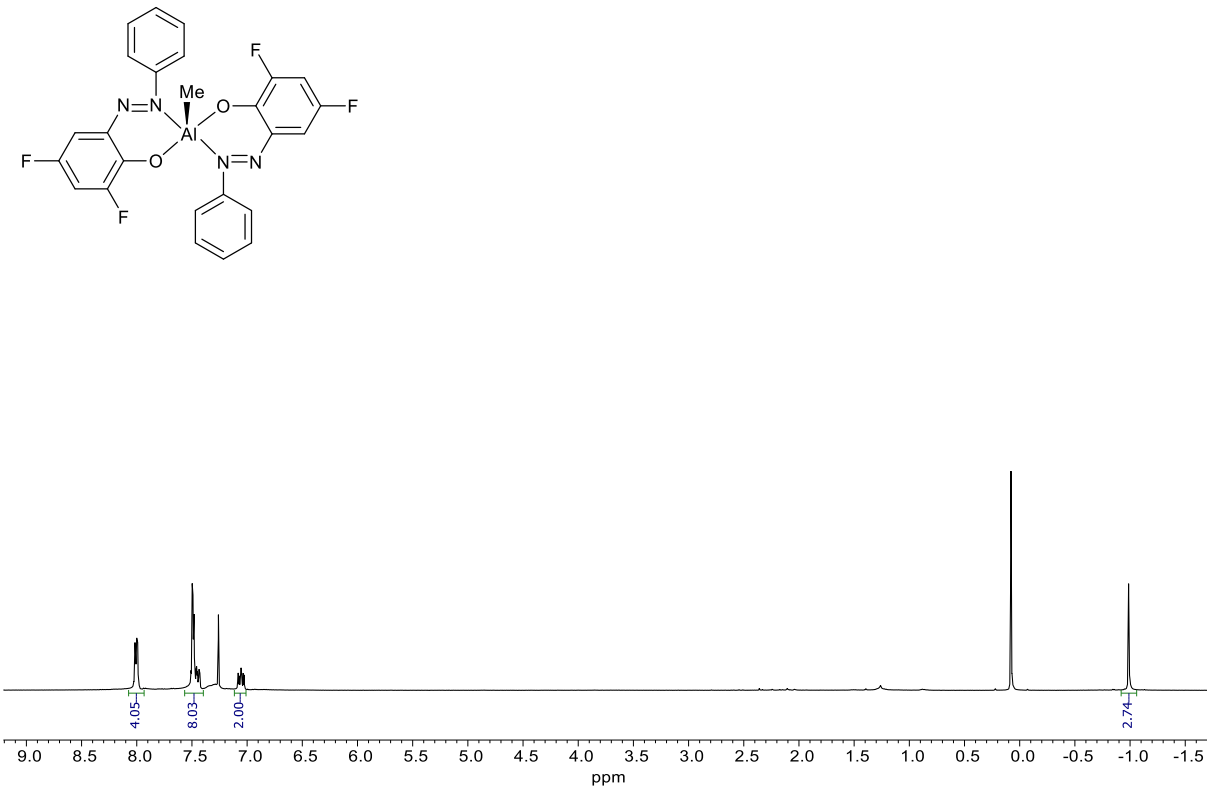

Fig. S16 ^{1}H NMR spectrum of **6b** in $CDCl_3$ at 298 K (* = solvent residue signal).

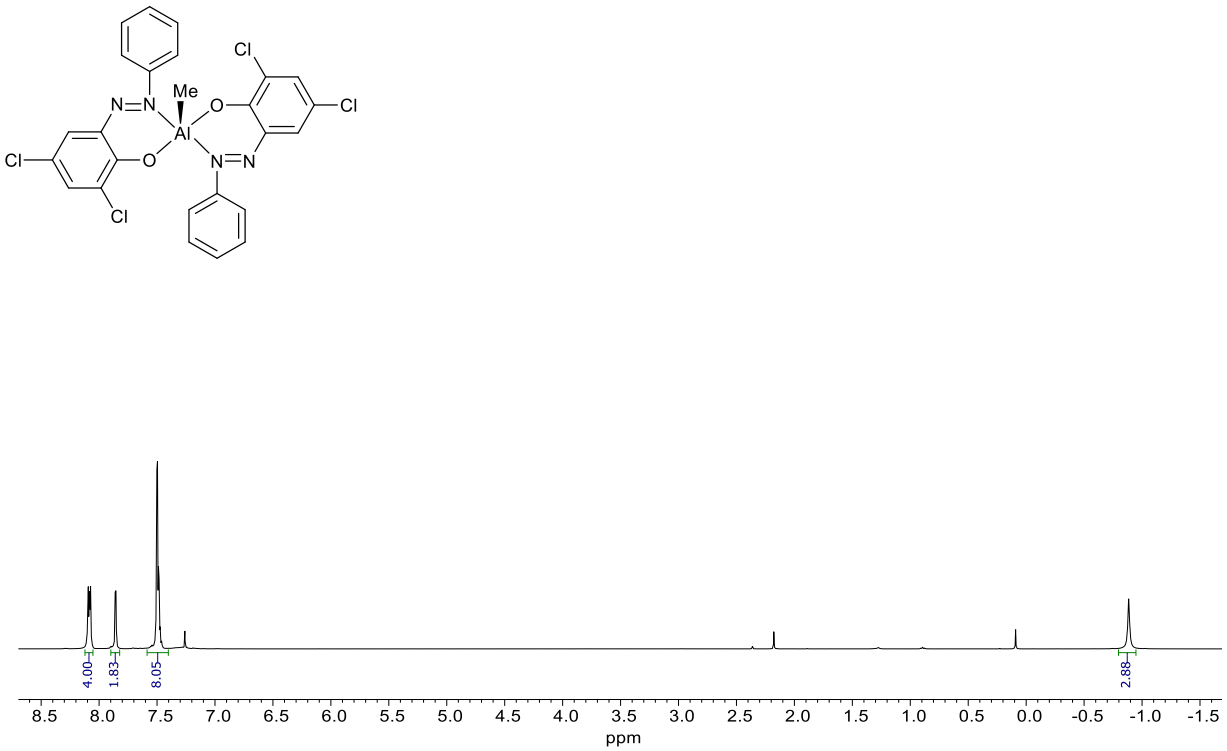

Fig. S17 ^{1}H NMR spectrum of **7b** in $CDCl_3$ at 298 K (* = solvent residue signal).

Table S1 Crystallographic data and structure refinement details for complex **4a**.

Crystal and refinement data	**Complex 4a**
Empirical formula	$C_{16}H_{19}AlN_2O$
Formula weight	282.31
Temperature/K	100
Crystal system	triclinic
Space group	P-1
a/Å	7.3646(6)
b/Å	9.4194(8)
c/Å	11.4053(10)
α/°	77.248(2)
β/°	80.825(2)
γ/°	82.816(2)
Volume/Å^3	758.47(11)
Z	2
ρ_{calc}g/cm^3	1.236
μ/mm^{-1}	1.139
F(000)	300.0
Crystal size/mm^3	0.15 × 0.15 × 0.15
Radiation	CuKα (λ = 1.54178)
2Θ range for data collection/°	9.67 to 144.268
Index ranges	$-9 \le h \le 9$, $-11 \le k \le 11$, $-14 \le l \le 13$
Reflections collected	11471
Independent reflections	2940 [R_{int} = 0.0223, R_{sigma} = 0.0219]
Data/restraints/parameters	2940/0/185
Goodness-of-fit on F^2	1.065
Final R indexes [I>=2σ (I)]	R_1 = 0.0314, wR_2 = 0.0825
Final R indexes [all data]	R_1 = 0.0316, wR_2 = 0.0826
Largest diff. peak/hole / e Å^{-3}	0.27/–0.27

Table S2 Bond lengths (Å) and bond angles (°) for complex **4a**.

Bond lengths (Å)

Al1-O1	1.7770(9)	C1-C2	1.3919(16)	C10-C11	1.3726(17)
Al1-N1	2.0012(10)	C1-C6	1.3943(16)	C11-C12	1.4114(17)
Al1-C7	1.9581(12)	C2-C3	1.3867(18)	C11-C15	1.5071(16)
Al1-C8	1.9568(13)	C3-C4	1.3945(18)	C12-C13	1.3816(17)
O1-C14	1.3214(14)	C4-C5	1.3819(17)	C13-C14	1.4138(16)
N1-N2	1.2852(14)	C5-C6	1.3977(17)	C13-C16	1.5050(16)
N1-C6	1.4358(14)	C9-C10	1.4182(16)		
N2-C9	1.3762(15)	C9-C14	1.4209(16)		

Bond angles (°)

O1-Al1-N1	93.45(4)	C2-C1-C6	119.75(11)	C9-C10-C11	121.41(11)
O1-Al1-C7	109.97(5)	C1-C2-C3	120.16(11)	C10-C11-C12	117.50(11)
O1-Al1-C8	111.69(5)	C2-C3-C4	119.5(2)	C10-C11-C15	122.09(11)
N1-Al1-C7	112.79(5)	C3-C4-C5	120.54(11)	C12-C11-C15	120.40(11)
N1-Al1-C8	107.98(5)	C4-C5-C6	119.58(11)	C11-C12-C13	123.51(11)
C7-Al1-C8	118.22(6)	N1-C6-C1	118.00(10)	C12-C13-C14	118.89(11)
Al1-O1-C14	127.99(7)	N1-C6-C5	121.84(10)	C12-C13-C16	122.17(10)
Al1-N1-N2	124.71(8)	C1-C6-C5	120.13(10)	C14-C13-C16	118.94(11)
Al1-N1-C6	122.07(8)	N2-C9-C10	112.94(10)	O1-C14-C9	121.85(10)
N2-N1-C6	113.02(9)	N2-C9-C14	127.04(10)	O1-C14-C13	119.45(10)
N1-N2-C9	121.98(10)	C10-C9-C14	119.99(10)	C9-C14-C13	118.69(10)

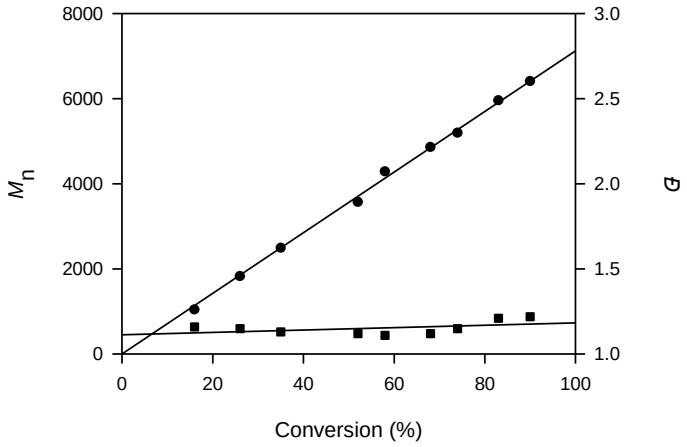

Fig. S18 Plot of PLA M_n (●) (versus polystyrene standards) and PDI (○) as a function of monomer conversion for a *rac*-LA polymerisation using **1b**/$PhCH_2OH$ ($[LA]_0/[Al] = 50$, toluene, 70 ºC).

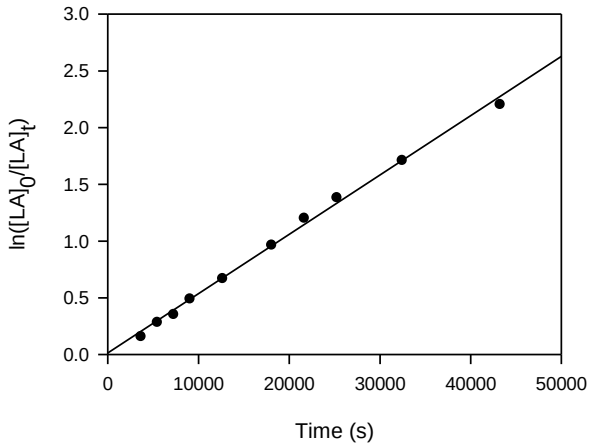

Fig. S19 Semilogarithmic plots of *rac*-lactide conversion *versus* time in toluene at 70 ºC wth complexes **1a** (●) ($[LA]_0/[Al]/[PhCH_2OH] = 50:1:1$, $[LA]_0 = 0.42$ M, [Al] = 8.33 mM).

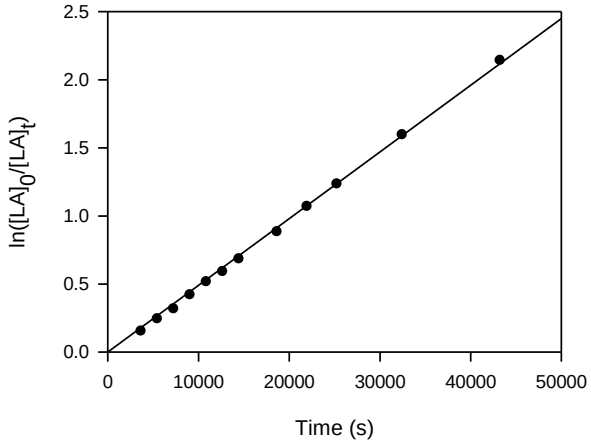

Fig. S20 Semilogarithmic plots of *rac*-lactide conversion *versus* time in toluene at 70 ºC with complex **2a** (●) ($[LA]_0/[Al]/[PhCH_2OH] = 50:1:1$, $[LA]_0 = 0.42$ M, [Al] = 8.33 mM).

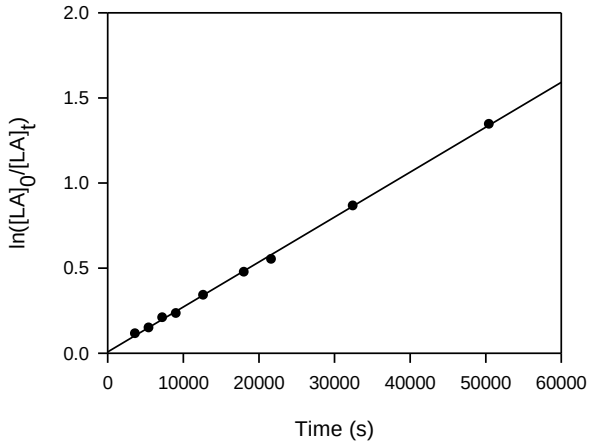

Fig. S21 Semilogarithmic plots of *rac*-lactide conversion *versus* time in toluene at 70 ºC with complex **4a** (●) ($[LA]_0/[Al]/[PhCH_2OH]$ = 50:1:1, $[LA]_0$ = 0.42 M, [Al] = 8.33 mM).

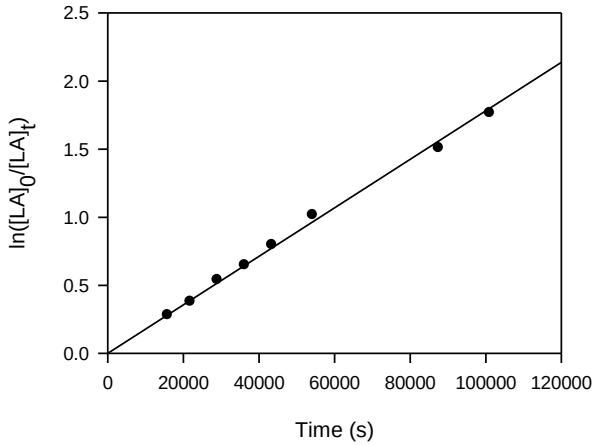

Fig. S22 Semilogarithmic plots of *rac*-lactide conversion *versus* time in toluene at 70 ºC with complex **5a** (●) ($[LA]_0/[Al]/[PhCH_2OH]$ = 50:1:1, $[LA]_0$ = 0.42 M, [Al] = 8.33 mM).

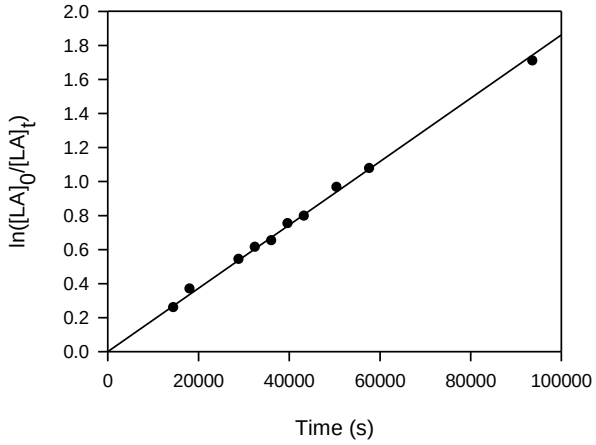

Fig. S23 Semilogarithmic plots of *rac*-lactide conversion *versus* time in toluene at 70 ºC with complexes **6a** (●) ($[LA]_0/[Al]/[PhCH_2OH]$ = 50:1:1, $[LA]_0$ = 0.42 M, [Al] = 8.33 mM).

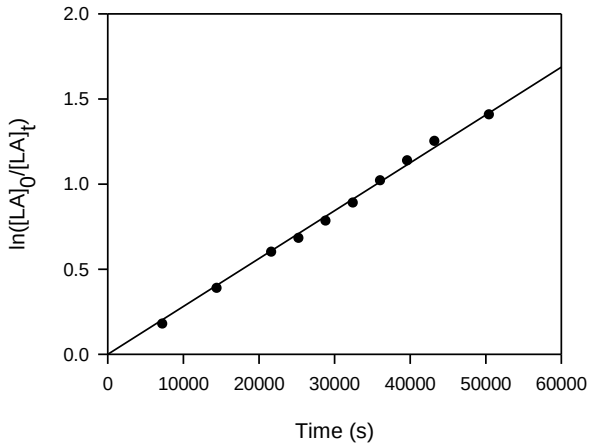

Fig. S24 Semilogarithmic plots of *rac*-lactide conversion *versus* time in toluene at 70 ºC with complex **7a** (●) ($[LA]_0/[Al]/[PhCH_2OH]$ = 50:1:1, $[LA]_0$ = 0.42 M, [Al] = 8.33 mM).

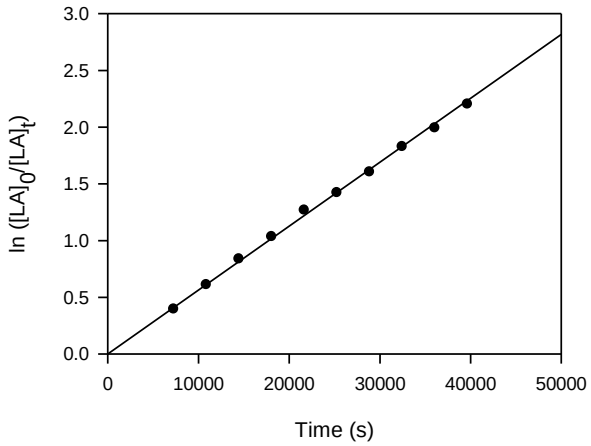

Fig. S25 Semilogarithmic plots of *rac*-lactide conversion *versus* time in toluene at 70 ºC with complexes **1b** (●) ($[LA]_0/[Al]/[BnOH]$ = 50:1:1, $[LA]_0$ = 0.42 M, [Al] = 8.33 mM).

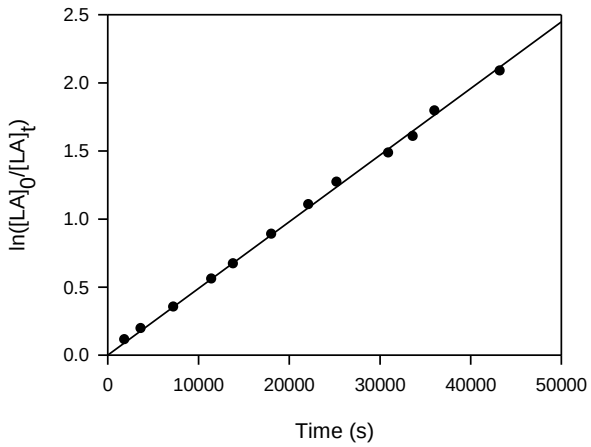

Fig. S26. Semilogarithmic plots of *rac*-lactide conversion *versus* time in toluene at 70 ºC with complex **2b** (●) ($[LA]_0/[Al]/[BnOH]$ = 50:1:1, $[LA]_0$ = 0.42 M, [Al] = 8.33 mM).

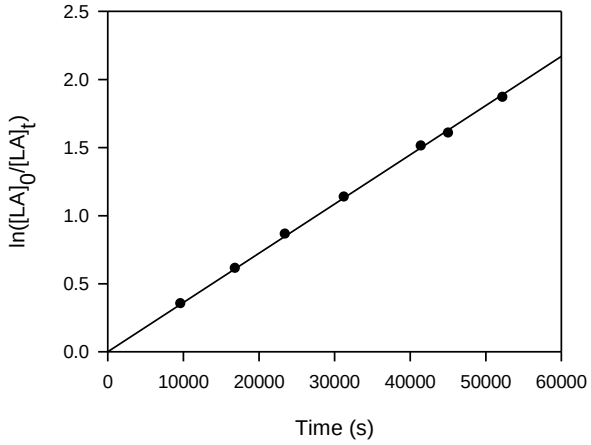

Fig. S27 Semilogarithmic plots of *rac*-lactide conversion *versus* time in toluene at 70 ºC with complex **3b** (●) ($[LA]_0/[Al]/[BnOH]$ = 50:1:1, $[LA]_0$ = 0.42 M, [Al] = 8.33 mM).

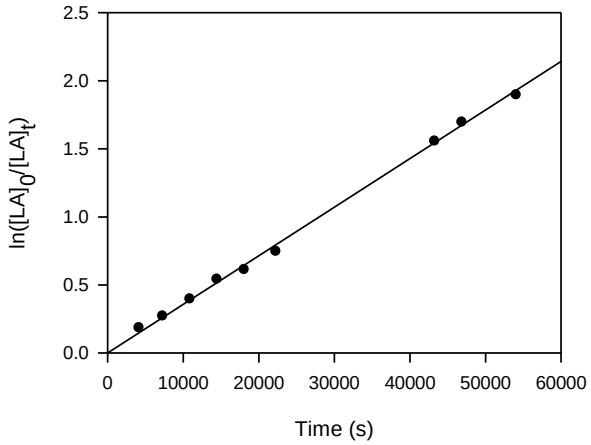

Fig. S28 Semilogarithmic plots of *rac*-lactide conversion *versus* time in toluene at 70 ºC with complex **4b** (●) ($[LA]_0/[Al]/[BnOH]$ = 50:1:1, $[LA]_0$ = 0.42 M, [Al] = 8.33 mM).

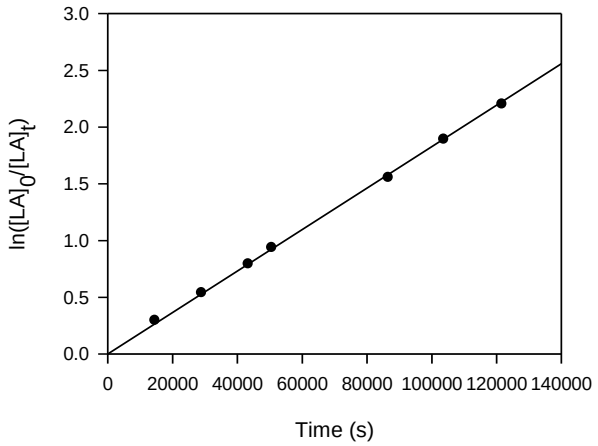

Fig. S29 Semilogarithmic plots of *rac*-lactide conversion *versus* time in toluene at 70 ºC with complex **5b** (●) ($[LA]_0/[Al]/[BnOH]$ = 50:1:1, $[LA]_0$ = 0.42 M, [Al] = 8.33 mM).

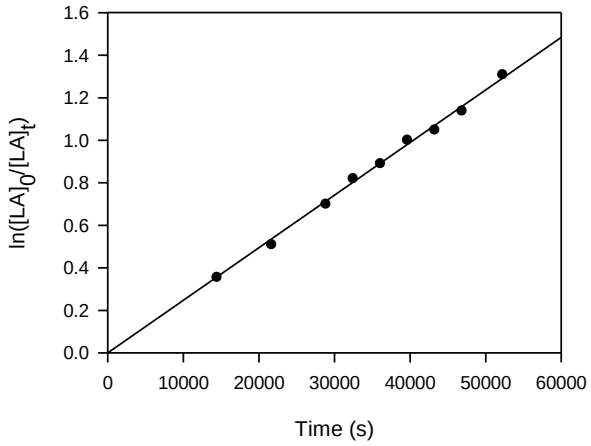

Fig. S30 Semilogarithmic plots of *rac*-lactide conversion *versus* time in toluene at 70 ºC with complex **6b** (●) ($[LA]_0/[Al]/[BnOH]$ = 50:1:1, $[LA]_0$ = 0.42 M, [Al] = 8.33 mM).

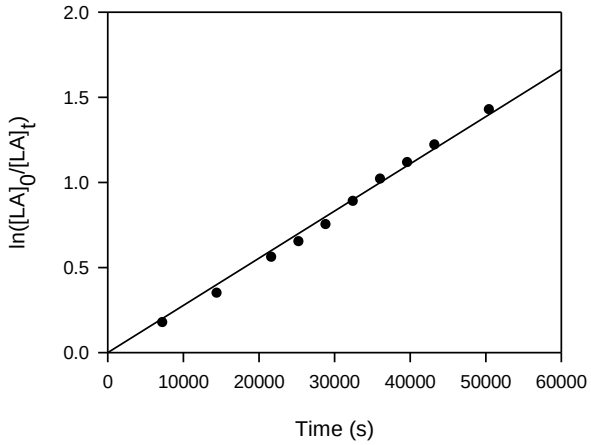

Fig. S31 Semilogarithmic plots of *rac*-lactide conversion *versus* time in toluene at 70 ºC with complex **7b** (●) ($[LA]_0/[Al]/[BnOH]$ = 50:1:1, $[LA]_0$ = 0.42 M, [Al] = 8.33 mM).

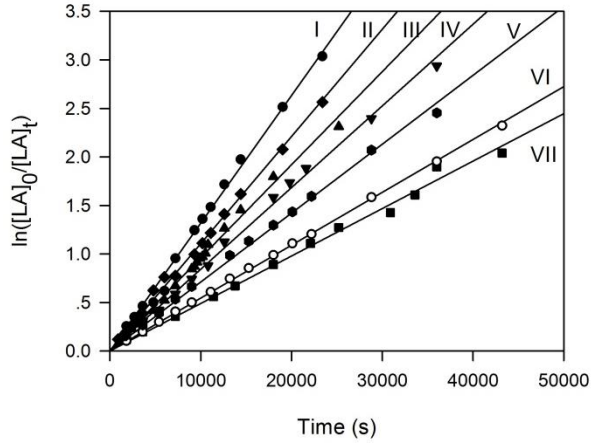

Fig. S32 Semilogarithmic plots of the *rac*-lactide conversion versus time in toluene at 70 °C with complex **2b**/BnOH as an initiator ($[LA]_0$ = 0.42 M: **I**, [Al] = 24.99 mM, $[LA]_0/[Al]$ = 17; **II**, [Al] = 20.82 mM, $[LA]_0/[Al]$ = 20; **III**, [Al] = 16.66 mM, $[LA]_0/[Al]$ = 25; **IV**, [Al] = 14.58 mM, $[LA]_0/[Al]$ = 29; **V**, [[Al] = 12.50 mM, $[LA]_0/[Al]$ = 34; **VI**, [Al] = 10.41 mM, $[LA]_0/[Al]$ = 40; **VII**, [Al] = 8.33 mM $[LA]_0/[Al]$ = 50).

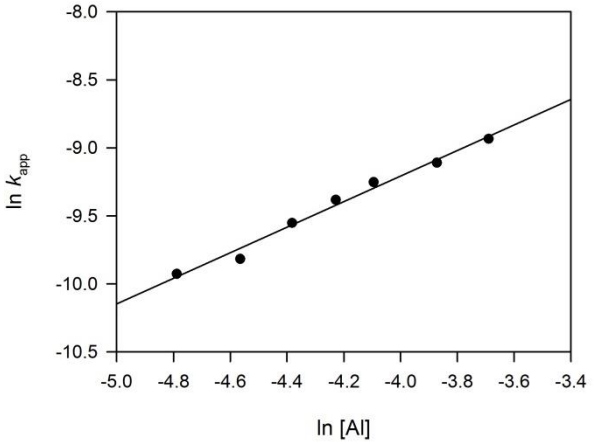

Fig. S33 Plot of ln k_{app} versus ln [Al] for the polymerisation of *rac*-lactide with complex **2b**/BnOH as an initiator (toluene, 70 °C, $[LA]_0$ = 0.42 M).

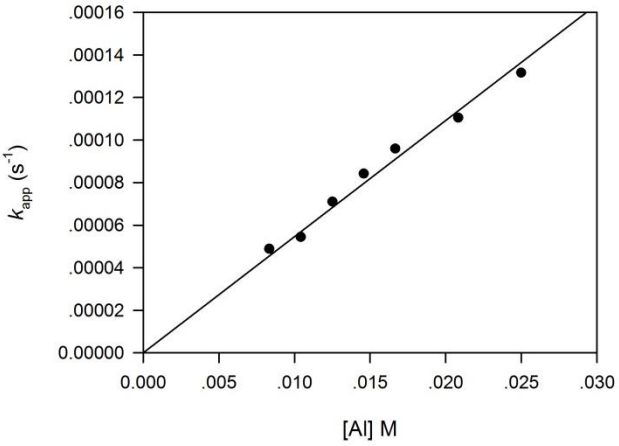

Fig. S34 Plot of k_{app} versus [Al] for the polymerisation of *rac*-lactide with complex **2b**/BnOH as an initiator (toluene, 70 °C, $[LA]_0$ = 0.42 M).

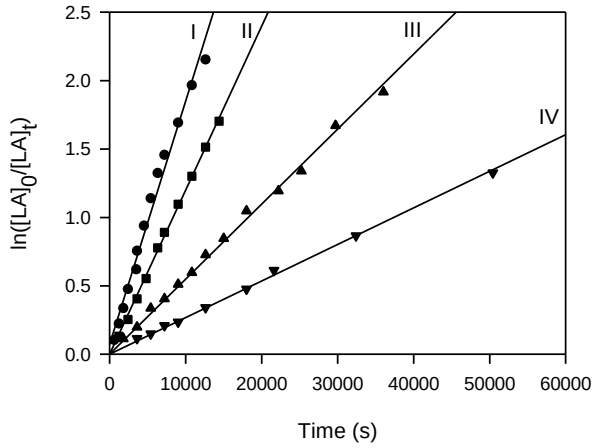

Fig. S35 Semilogarithmic plots of the *rac*-lactide conversion versus time in toluene with complex **4a**/BnOH as an initiator at **I**, 100 °C, k_{app} = (18.71 ± 0.43) × 10^{-5} s^{-1}; **II**, 90°C, k_{app} = (11.99 ± 0.13) × 10^{-5} s^{-1}; **III**, 80°C, k_{app} = (5.48 ± 0.06) × 10^{-5} s^{-1} ; **IV**, 70°C, k_{app} = (2.71 ± 0.04) × 10^{-5} s^{-1} ($[LA]_0$ = 0.42 M, [Al] = 8.33 mM $[LA]_0$/[Al] = 50).

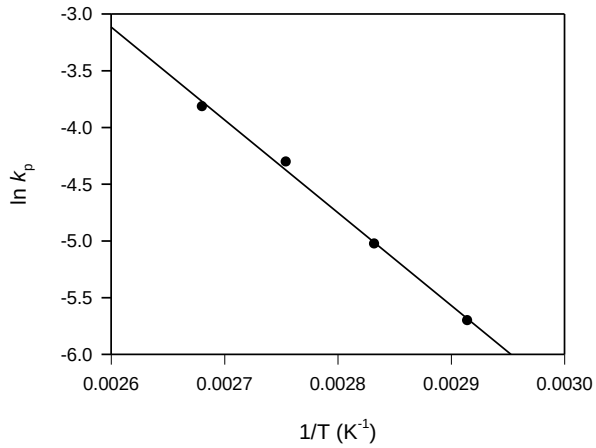

Fig. S36 Arrhenius plot of ln k_p *versus* 1/T for the polymerisation of *rac*-LA with **4a**/BnOH as an initiator ($[LA]_0$/[Al] = 50, $[LA]_0$ = 0.42 M, toluene)**.**

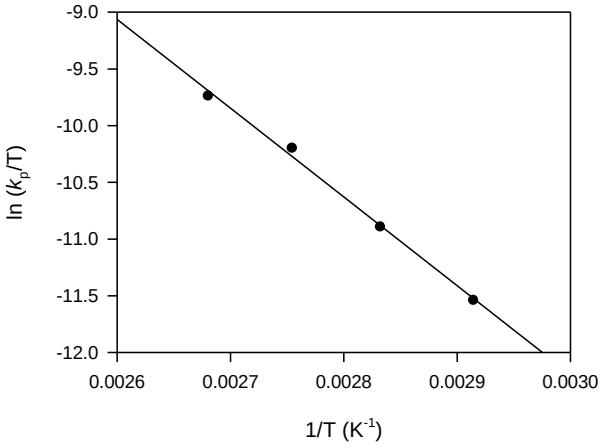

Fig. S37 Eyring plot of ln (k_p/T) *versus* 1/T for the polymerisation of *rac*-LA with **4a**/BnOH as an initiator ($[LA]_0$/[Al] = 50, $[LA]_0$ = 0.42 M, toluene)**.**

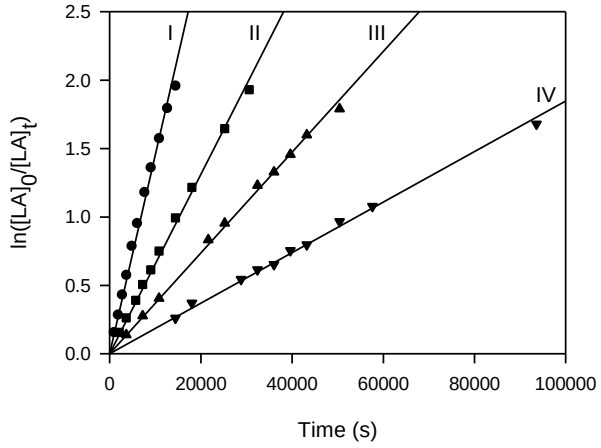

Fig. S38 Semilogarithmic plots of the *rac*-lactide conversion versus time in toluene with complex **6a**/BnOH as an initiator at **I**, 100 °C, k_{app} = (14.54 ± 0.30) × 10^{-5} s^{-1}; **II**, 90°C, k_{app} = (6.30 ± 0.10) × 10^{-5} s^{-1}; **III**, 80°C, k_{app} = (3.68 ± 0.03) × 10^{-5} s^{-1} ; **IV**, 70°C, k_{app} = (1.87 ± 0.02) × 10^{-5} s^{-1} ($[LA]_0$ = 0.42 M, [Al] = 8.33 mM $[LA]_0$/[Al] = 50).

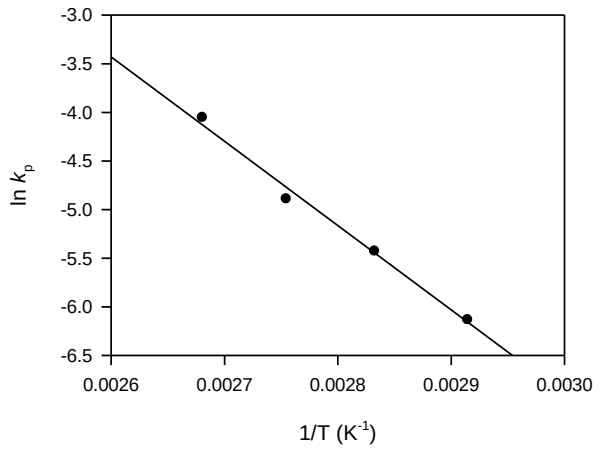

Fig. S39 Arrhenius plot of ln k_p *versus* 1/T for the polymerisation of *rac*-LA with **6a**/BnOH as an initiator ($[LA]_0$/[Al] = 50, $[LA]_0$ = 0.42 M, toluene)**.**

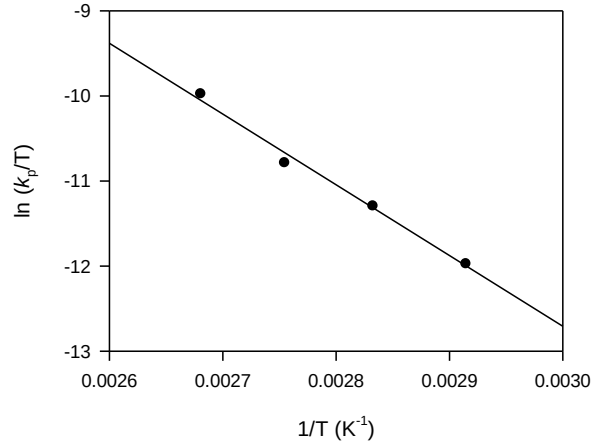

Fig. S40 Eyring plot of ln (k_p/T) *versus* 1/T for the polymerisation of *rac*-LA with **6a**/BnOH as an initiator ($[LA]_0$/[Al] = 50, $[LA]_0$ = 0.42 M, toluene)**.**

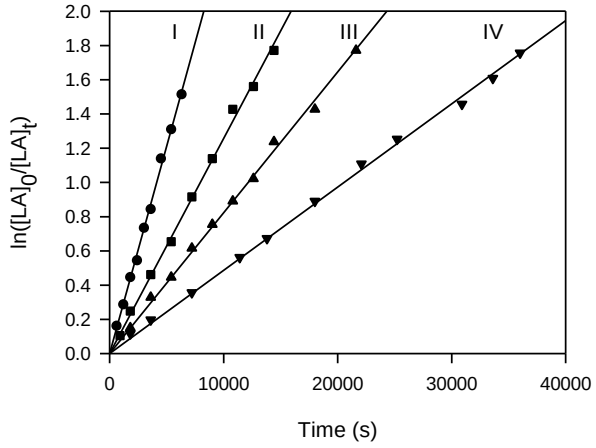

Fig. S41 Semilogarithmic plots of the *rac*-lactide conversion *versus* time in toluene with complex **2b**/BnOH as an initiator at **I**, 100 °C, k_{app} = (24.23 ± 0.29) × 10^{-5} s^{-1}; **II**, 90°C, k_{app} = (12.60 ± 0.08) × 10^{-5} s^{-1}; **III**, 80°C, k_{app} = (8.10 ± 0.14) × 10^{-5} s^{-1} ; **IV**, 70°C, k_{app} = (4.90 ± 0.06) × 10^{-5} s^{-1} ($[LA]_0$ = 0.42 M, [Al] = 8.33 mM $[LA]_0$/[Al] = 50).

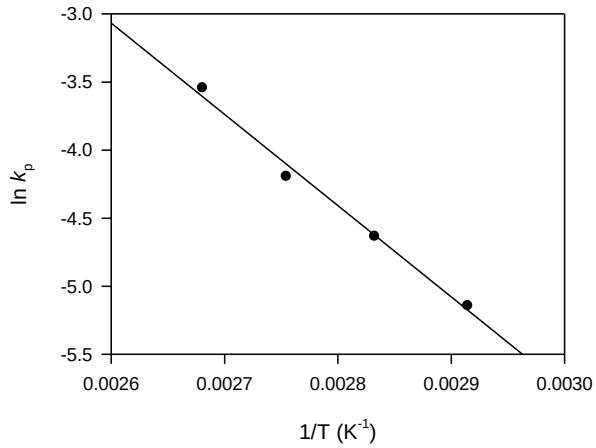

Fig. S42 Arrhenius plot of ln k_p *versus* 1/T for the polymerisation of *rac*-LA with **2b**/BnOH as an initiator ($[LA]_0$/[Al] = 50, $[LA]_0$ = 0.42 M, toluene)**.**

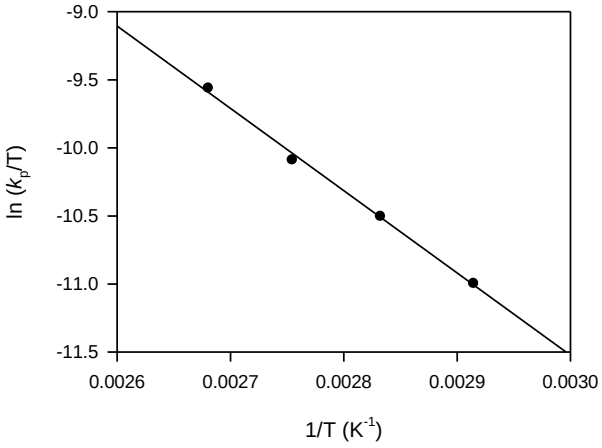

Fig. S43 Eyring plot of ln (k_p/T) *versus* 1/T for the polymerisation of *rac*-LA with **2b**/BnOH as an initiator ($[LA]_0$/[Al] = 50, $[LA]_0$ = 0.42 M, toluene)**.**

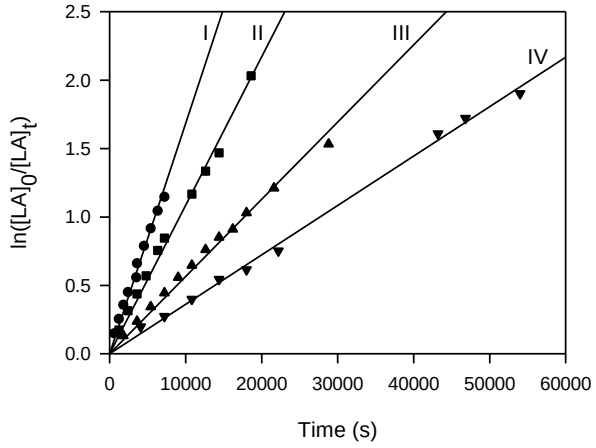

Fig. S44 Semilogarithmic plots of the *rac*-lactide conversion *versus* time in toluene with complex **4b**/BnOH as an initiator at **I**, 100 °C, k_{app} = (16.83 ± 0.54) × 10^{-5} s^{-1}; **II**, 90°C, k_{app} = (10.85 ± 0.27) × 10^{-5} s^{-1}; **III**, 80°C, k_{app} = (5.64 ± 0.15) × 10^{-5} s^{-1} ; **IV**, 70°C, k_{app} = (3.64 ± 0.08) × 10^{-5} s^{-1} ($[LA]_0$ = 0.42 M, [Al] = 8.33 mM $[LA]_0$/[Al] = 50).

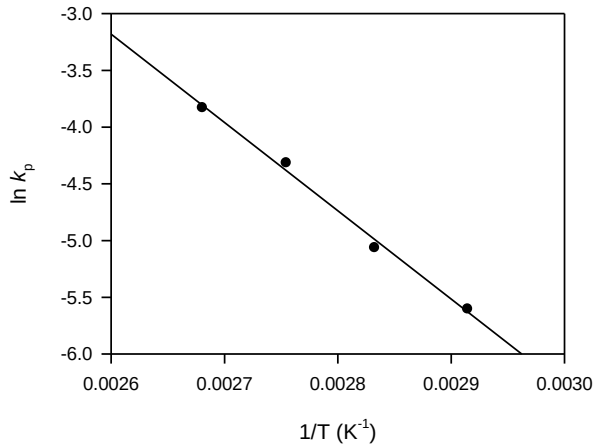

Fig. S45 Arrhenius plot of ln k_p *versus* 1/T for the polymerisation of *rac*-LA with **4b**/BnOH as an initiator ($[LA]_0$/[Al] = 50, $[LA]_0$ = 0.42 M, toluene)**.**

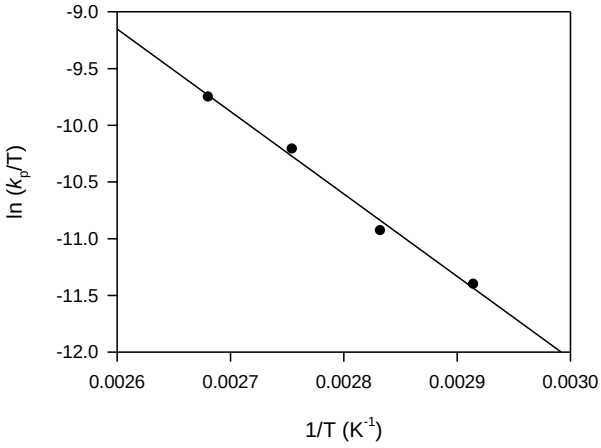

Fig. S46 Eyring plot of ln (k_p/T) *versus* 1/T for the polymerisation of *rac*-LA with **4b**/BnOH as an initiator ($[LA]_0$/[Al] = 50, $[LA]_0$ = 0.42 M, toluene)**.**

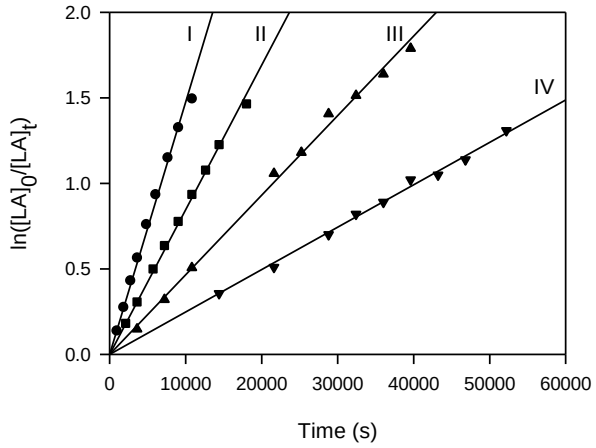

Fig. S47 Semilogarithmic plots of the *rac*-lactide conversion *versus* time in toluene with complex **6b**/BnOH as an initiator at **I**, 100 °C, k_{app} = (14.74 ± 0.26) × 10^{-5} s^{-1}; **II**, 90°C, k_{app} = (8.46 ± 0.08) × 10^{-5} s^{-1}; **III**, 80°C, k_{app} = (4.61 ± 0.05) × 10^{-5} s^{-1} ; **IV**, 70°C, k_{app} = (2.48 ± 0.02) × 10^{-5} s^{-1} ($[LA]_0$ = 0.42 M, [Al] = 8.33 mM $[LA]_0$/[Al] = 50).

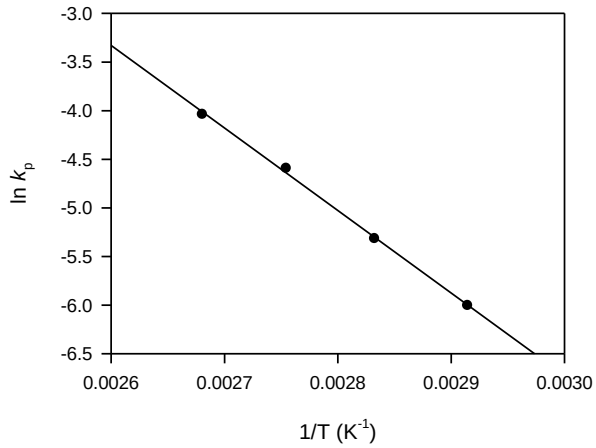

Fig. S48 Arrhenius plot of ln k_p *versus* 1/T for the polymerisation of *rac*-LA with **6b**/BnOH as an initiator ($[LA]_0$/[Al] = 50, $[LA]_0$ = 0.42 M, toluene)**.**

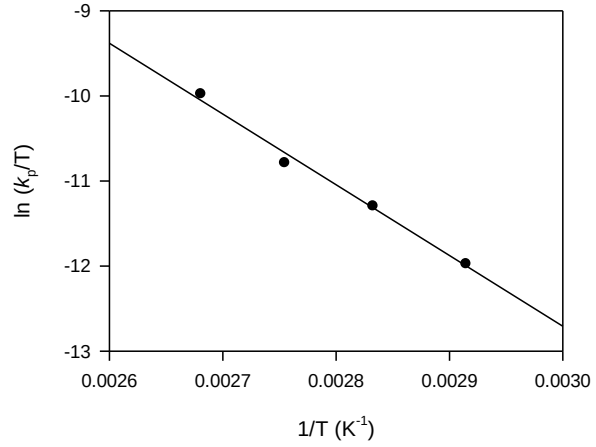

Fig. S49 Eyring plot of ln (k_p/T) *versus* 1/T for the polymerisation of *rac*-LA with **6b**/BnOH as an initiator ($[LA]_0$/[Al] = 50, $[LA]_0$ = 0.42 M, toluene)**.**

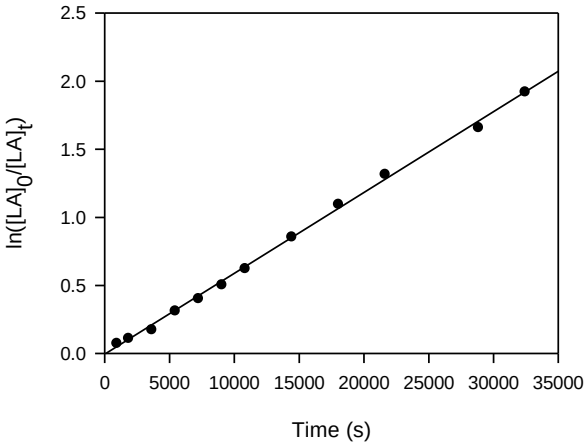

Fig. S50 Semilogarithmic plots of *rac*-lactide conversion *versus* time in toluene at 70 ºC with complex **8a** (●) ($[LA]_0/[Al]/[BnOH]$ = 50:1:1, $[LA]_0$ = 0.42 M, [Al] = 8.33 mM).

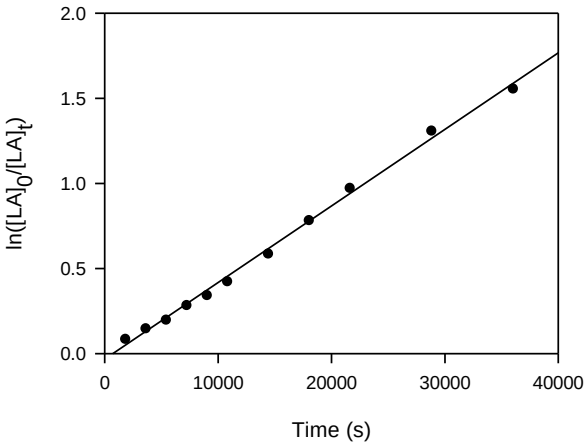

Fig. S51 Semilogarithmic plots of *rac*-lactide conversion *versus* time in toluene at 70 ºC with complex **8b** (●) ($[LA]_0/[Al]/[BnOH]$ = 50:1:1, $[LA]_0$ = 0.42 M, [Al] = 8.33 mM).